

Table V. Heats of Formation of Pyridine-Type Compounds in kcal/mol

compound	ΔH_f , calcd	ΔH_f , expt	difference
pyridine	32.1	34.55	-2.5
pyrazine	47.7	46.90	0.8
pyrimidine	47.0	47.00	0.0
isoquinoline	47.3	48.20	-0.9
quinoline	46.6	51.80	-5.2
quinoxaline	61.2	62.70	-1.5
phenazine	80.9	80.70	0.2
7,8-benzoquinoline	55.2	55.19	0.0
5,6-benzoquinoline	61.1	55.90	5.2
3,4-benzoquinoline	60.2	58.20	2.0
acridine	65.6	69.90	-4.3

Conclusions

While conjugated hydrocarbons were successfully dealt with by molecular mechanics years ago, the introduction of heteroatoms poses special problems. Firstly, information vital to good parameterization, such as, accurate structures, rotational barriers, heats of formation, dipole moments, etc., is very scarce for heterocycles. There are not enough model compounds to allow for unique choices of parameters. Secondly, polarization becomes important, and there is no simple way for dealing with it at present. But since heterocycles are so important, we have taken the first step of providing a scheme to include them in the present framework of MM2. Polarization is not explicitly taken care of. Only heterocycles including nitrogen atoms are reported here, although the same scheme can handle other heteroatoms as well. As we have already shown, the agreement between the calculated structures and the experimental ones is generally good. However, an attempt at predicting the heats of formation yielded disappointing results. We believe that the failure to calculate accurate

heats of formation and the dipole moments of azulene and linear conjugated amines is in large part due to our neglect of the polarization in the π system.²³ Preliminary studies employing the variable electronegativity self-consistent field molecular orbitals rather than the self-consistent field molecular orbitals as used here showed great improvement in predicting the dipole moments of azulene and of conjugated ketones.²⁴ We think that as better and more abundant experimental data on conjugated heterocycles become available, it will be worthwhile to reexamine the method presented in this work.

Acknowledgment. We are indebted to Professor K. N. Trueblood for a copy of his current program for correcting crystallographic bond lengths for rigid body motion. We are also indebted to the National Institutes of Health (5 R24 RR02165) and the National Science Foundation (CHE 8315543) for support of this work.

Supplementary Material Available: Experimental and calculated data and structures for compounds listed in this paper (48 pages). Ordering information is given on any current masthead page.

(23) Experimental error may also be a problem. We have been advised (personal communication to N.L.A. by W. Steele) that his repeated determinations of the heats of formation of several heterocycles have given values which differ from those reported earlier by more than the quoted error limits would suggest.

(24) A referee has suggested that if nonneighbor resonance integrals are included in the π system calculation, the polarization in the π system will be represented differently, and this may improve the dipole moments. This may well be true, but the whole π system calculation, beginning with hydrocarbons (ref 5) has been parameterized without including these integrals. It is not possible to add them in an ad hoc fashion now. One would have to go back and reparameterize the whole calculation. This was not done originally, because the earlier work on heats of formation was not parameterized in this fashion.

Photophysical Properties of Fluorescent *N*-Purin-6-ylpyridinium Chloride[†]

B. Skalski, R. P. Steer,* and R. E. Verrall*

Contribution from the Department of Chemistry, University of Saskatchewan, Saskatoon, Canada S7N 0W0. Received May 26, 1987

Abstract: The absorption and fluorescence spectra and the excited-state lifetimes of *N*-purin-6-ylpyridinium chloride have been studied in polar organic solvents (acetonitrile, methanol, and ethanol) and, as a function of pH, in water. The ground state exhibits a prototropic equilibrium between the cation and the zwitterion with $pK_a = 6.7$ in H₂O. At 3 < pH < 6 in aqueous solutions, excitation of the ground-state cation results in proton transfer to give only the excited zwitterion, on a time scale that is short compared to the lifetime of the excited species. A large Stokes shift in the emission results. The fluorescence quantum yield and lifetime of the excited zwitterion are 0.08 and 1.6 ns, respectively, in aqueous solution and remain constant over the entire 3 < pH < 9 range. Diabatic proton transfer to the excited zwitterion at pH < 3 results in quenching of the emission with a rate constant of $2 \times 10^9 \text{ M}^{-1} \text{ s}^{-1}$. Proton quenching does not dominate the excited zwitterion decay, however, so that the apparent pK_a^* values of 0.4 ± 0.3 from the Förster cycle and 0.6 ± 0.1 from fluorescence titration give good approximations to the true excited state pK_a^* . The effects of solvent and temperature have also been examined. The potential application of pyridinium salts of purines as fluorescence probes for biomolecules is discussed.

Purines and related compounds are widely distributed among natural products. In particular, a vast body of information is now available concerning the roles that these molecules play in the chemistry and physics of nucleic acids and other biomolecules.¹ The use of luminescence techniques to probe the structure and dynamic behavior of macromolecules such as these continues to provide some of the most useful data available.²⁻⁴

The purines form part of the near-UV light-absorbing system in nucleic acids. However, the use of purine moieties as lumi-

(1) Shaw, G. In *Comprehensive Heterocyclic Chemistry*; Katritzky, A. R., Rees, C. W., Eds.; Pergamon: New York, 1984; Vol. 5 p 499 ff.

(2) McCammon, A.; Karplus, M. *Acc. Chem. Res.* 1983, 16, 187. Andreoni, A.; Sacchi, C. A.; Svelto, O. In *Chemical and Biochemical Applications of Lasers*; Moore, C. B., Ed.; Academic: New York, 1979; Vol. IV, p 1.

(3) Eisinger, J.; Lamola, A. A. In *Excited States of Proteins and Nucleic Acids*; Steiner, R. F., Weinryb, I., Eds.; Plenum: New York, 1971; p 107 ff.

[†]Preliminary results were presented at the 69th Annual Conference of the Chemical Institute of Canada, Saskatoon, June 1986.

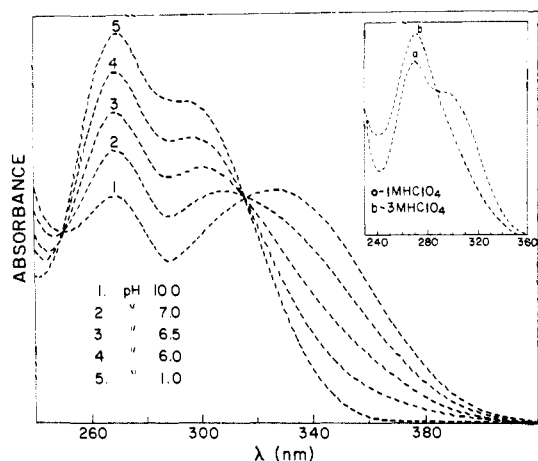


Figure 1. Absorption spectra of *N*-purin-6-ylpyridinium chloride at different pHs. Inset, a comparison of the spectra in 1 M and 3 M HClO₄.

nescent probes is limited by the fact that, like most common bases of DNA and RNA, the neutral species fluoresce weakly ($\phi_f \leq 10^{-4}$) in room-temperature aqueous solutions at physiological pHs.³ In addition, intramolecular energy transfer from excited purines to weakly luminescent pyrimidines can also occur when the two bases are present in the same polynucleotide.⁴ Although some protonated purines do fluoresce from room-temperature solutions, this fluorescence is suppressed when the 9-position is substituted, as in their nucleotides.⁵ Both fluorescence and phosphorescence⁶ can be observed in frozen aqueous solutions at 77 K, but the difficulties in interpreting the results of such experiments are well-known.³ The desirability of synthesizing a substituted purine that fluoresces strongly in aqueous solutions at room temperature is evident.

Adamiak et al.^{7,8} have recently reported that nucleic acid bases such as hypoxanthine, guanine, uracil, thymine, and their O-protected nucleosides undergo a quantitative transformation into water-soluble, fluorescent pyridinium salts when treated with various phosphorylating agents in the presence of pyridine. Apart from the importance of these compounds with respect to side processes in nucleic acid synthesis⁸ and other synthetic applications,⁹ they have also become the subject of interesting photochemical¹⁰ and photophysical investigations. Of particular interest is the possibility of using these compounds and especially their photochemical transformants¹⁰ as fluorescent, molecular probes.

N-Purin-6-ylpyridinium chloride (PuPyCl) has been identified as a major product of the photolysis of an acidic aqueous solution of *N*-[9-(2',3',5'-tri-*O*-acetyl- β -D-ribofuranosyl)purin-6-yl]pyridinium chloride.¹⁰ Unlike the other members of the family of hypoxanthine-derived pyridinium salts, this compound appears to be photostable in water. It exhibits an anomalously large Stokes shift (~ 230 nm) in its emission spectrum, perhaps indicative of an excited-state proton transfer.^{8,9} The formation of a photostable, fluorescent zwitterion appears likely.

All of the above observations suggest that the pyridinium salts might find utility as fluorescent probes in purine-containing biomolecules. In this paper, the first of a series in which we explore this possibility in detail, we report the results of the base line spectroscopic and photophysical studies of PuPyCl in aqueous and nonaqueous solutions.

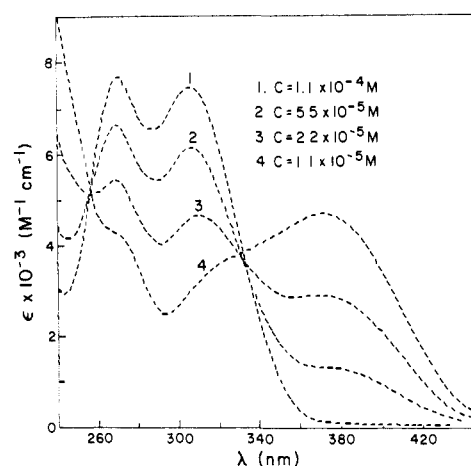


Figure 2. Concentration dependence of the absorption spectra of *N*-purin-6-ylpyridinium chloride in acetonitrile.

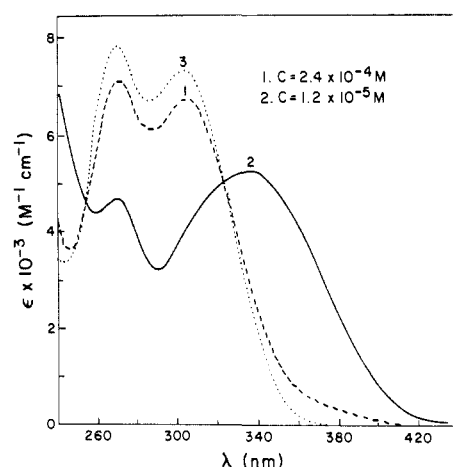


Figure 3. Concentration dependence of the absorption spectra of *N*-purin-6-ylpyridinium chloride in methanol. Curve 3 is for the same solution as 2 after acidifying to pH 3.5.

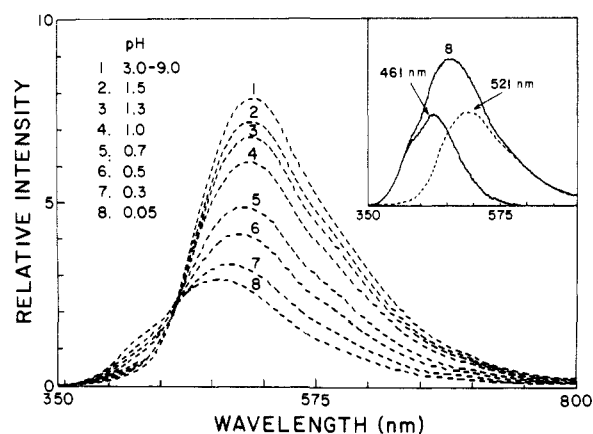


Figure 4. The pH dependence of the fluorescence spectra of PuPy⁺. Inset, the low-pH spectrum deconvoluted into the emission of the zwitterion ($\lambda_{\max} = 521$ nm) and cation ($\lambda_{\max} = 461$ nm).

Results and Discussion

1. UV Absorption Spectra. The UV absorption spectrum of PuPy⁺ is characterized by two overlapping, relatively strong $\pi \rightarrow \pi^*$ transitions in the 250–350-nm range. Depending upon the nature of the solvent, either the two bands are partially separated or the first appears as a shoulder on the low-energy side of the second (cf. Figures 1–3). The lower energy transition, which undergoes a blue shift in water compared to acetonitrile or methanol, results from strong intramolecular charge transfer (CT) between the two coplanar¹¹ π -electronic systems, i.e. between the

(4) Hauswirth, W. W.; Daniels, M. In *Photochemistry and Photobiology of Nucleic Acids*; Wang, S. Y., Ed.; Academic: New York, 1976; p 110 ff.

(5) Eisinger, J. *Photochem. Photobiol.* **1968**, *7*, 597. Borreson, H. C. *Acta Chem. Scand.* **1967**, *21*, 2463.

(6) Aaron, J. J.; Winefordner, J. D. *Photochem. Photobiol.* **1973**, *18*, 97.

(7) Adamiak, R. W.; Biala, E.; Skalski, B. *Nucleic Acids Res.* **1985**, *13*, 2989.

(8) Adamiak, R. W.; Biala, E.; Gdaniec, L.; Mielewczyk, S.; Skalski, B. *Chem. Scr.* **1986**, *26*, 3; **1986**, *26*, 7.

(9) Adamiak, R. W.; Biala, E.; Skalski, B. *Angew. Chem., Int. Ed. Engl.* **1985**, *24*, 1054.

(10) Skalski, B.; Adamiak, R. W.; Paszyc, S. *Nucleic Acids Symp. Ser.* **1984**, *14*, 293. Skalski, B.; Bartoszewicz, J.; Paszyc, S.; Gdaniec, Z.; Adamiak, R. *Tetrahedron* **1987**, *43*, 3955.

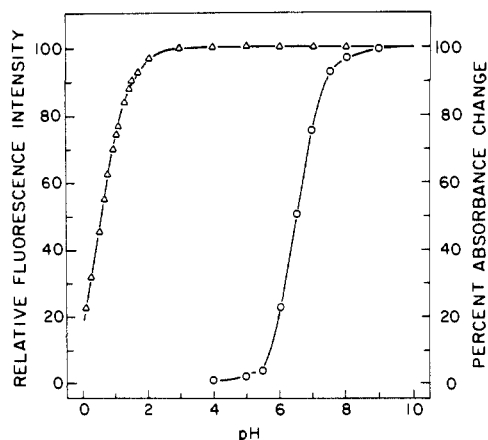


Figure 5. Titration curves of PuPy⁺: (O) % absorbance, and (Δ) fluorescence intensity (of the zwitterion only) vs pH.

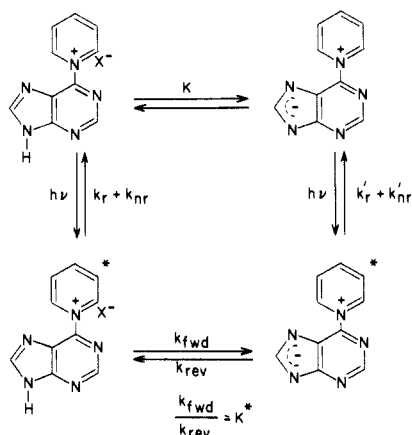


Figure 6. The ground and excited singlet state reactions of PuPy⁺ in aqueous solution with varying pH.

purine moiety (donor) and the positively charged pyridinium ring (acceptor). The higher energy transition, whose absorption maximum at $\lambda = 270$ nm is neither solvent nor pH sensitive, can be assigned to excitation within the pyridinium π -electronic system, by analogy with other similar molecules.¹²

The pH dependence of the absorption spectrum of PuPy⁺ is shown in Figure 1. With increasing pH, the CT absorption with $\lambda_{\max} = 294$ nm shifts gradually to longer wavelengths, and at pH > 8 a new band appears with $\lambda_{\max} = 325$ nm. The two isosbestic points at $\lambda = 250$ and 316 nm indicate the occurrence of a ground-state prototropic equilibrium in solution. Thus, it was concluded that the spectra at pH < 6 are associated with absorption by the cationic form of PuPy⁺ whereas those at pH > 8 are due to the zwitterion formed as a result of deprotonation of the nitrogen at the 9-position of the purine ring (cf. Figure 6). The ground-state pK_a (acidic) value for the dissociation of the 9-NH of PuPy⁺ obtained by spectrophotometric titration¹³ (cf. Figure 5) is equal to 6.7. This is approximately 2 orders of magnitude lower than that for the unsubstituted purine ($pK_a = 8.93$),¹⁶ reflecting the electron-withdrawing effect of the pyridinium substituent. This interpretation is consistent with the disappearance of the CT band in 3 M HClO₄ (insert, Figure 1), which is a consequence of the addition of a proton to the purine ring to form a dication and the elimination of interring charge transfer (vide infra).

Table I. UV Absorption Data for *N*-Purin-6-ylpyridinium Chloride in Various Solvents

solvent	dominant species	λ_{\max} (ϵ), nm ($M^{-1} \text{ cm}^{-1}$)	λ_{\max} (ϵ), nm ($M^{-1} \text{ cm}^{-1}$)
H ₂ O (pH 1)	cation	270 (9000)	292 (7500), sh
H ₂ O (pH 10)	zwitterion	269 (5400)	325 (5500)
CH ₃ OH (<i>c</i> , 1.9×10^{-4} M)	cation	272 (7800)	308 (7300)
CH ₃ OH (<i>c</i> , 8.9×10^{-6} M)	zwitterion	272 (4600)	341 (5200)
CH ₃ CN (<i>c</i> , 1.1×10^{-4} M)	cation	270 (7700)	306 (7500)
CH ₃ CN (<i>c</i> , 1.1×10^{-5} M)	zwitterion	270 (4300), sh	372 (4800)

In nonaqueous solvents such as acetonitrile and methanol, the absorption spectra exhibit a solute concentration dependence that is very similar to the observed pH dependence in water (see Figures, 2 and 3 and compare with Figure 1). Decreasing the concentration of the solute results in a large red shift of the CT absorption, and plots of the molar extinction coefficient ϵ vs λ show clear isosbestic points at $\lambda = 256$ and 326 nm in methanol and at $\lambda = 256$ and 334 nm in acetonitrile. This behavior is independent of the amount of added water up to 0.5% (ca. 0.3 M); however, no such concentration dependence is observed in slightly acidified acetonitrile and methanol solutions. We therefore conclude that the changes in the spectra of the unacidified nonaqueous solutions (Figures 2 and 3) are due to proton-transfer reactions similar to that found in water. The effects become observable in nonaqueous solution as a result of the increasing fraction of the cation which dissociates with decreasing solute concentration, as is usual for weak acids in dilute solution. Thus, the absorptions in methanol and acetonitrile at low solute concentration ($c < 10^{-5}$ M) can be attributed to the deprotonated, zwitterionic form of PuPy⁺.

The parameters characterizing the UV absorption of PuPy⁺ are summarized in Table I. It is interesting to note that the position of the CT absorption (especially of the zwitterion) depends on both the polarity and the proton-donating ability of the solvent. In polar, aprotic acetonitrile, the maximum is substantially redshifted compared to methanol. Similar behavior is observed in other heterocyclic compounds such as tertiary amine *N*-oxides and betaine-type structures⁸ and is indicative of the greater polarity and hydrogen-bonding (proton-accepting) ability of the ground state relative to the excited state. We conclude that the blue shift of the CT band of the zwitterion in going from acetonitrile to methanol to water reflects increasing stabilization of the ground state with increasing polarity and proton-donating ability of the solvent.

2. Fluorescence Spectra and Decay Times in Aqueous Solution. The emission spectrum of *N*-purin-6-ylpyridinium chloride in water is characterized by a single, rather broad band with a maximum at 521 nm. In contrast to absorption, the emission spectrum does not show any change over a wide pH range (pH 3–9, cf. Figure 4). Over this pH range, the excited-state luminescence decay is well-characterized by a single exponential function, with a lifetime of 1.6 ns.

The phosphorescence of triplet cationic, neutral, and anionic purine and several of its derivatives in rigid aqueous solutions at 77 K has previously been observed by Aaron and Winefordner.⁶ The phosphorescence spectra bear no resemblance to the present emission spectra, and both the radiative lifetime (vide infra) and spectral distribution of the emission in the PuPy⁺ system suggest that it is attributable to fluorescence from the lowest excited singlet (CT) state.

Both a comparison of the absorption and fluorescence spectra and the anomalously large Stokes shift suggest that the fluorescence within the pH 3–9 range originates from the zwitterionic form of excited PuPy⁺. Because the ground state exists almost exclusively in the monocationic form at $1 < \text{pH} < 6$ ($pK_a = 6.7$ for PuPy⁺ in its ground state) and because the fluorescence excitation spectra (not shown) replicate the corresponding absorption spectra exactly, the zwitterionic must be formed as a result of proton transfer from the cation to the solvent within the excited state's lifetime. This suggestion is supported by the large observed deuterium isotope effect, manifested as nearly twofold increases

(11) Jaskolski, M.; Skalski, B.; Adamiak, D. A.; Adamiak, R. W., submitted for publication in *Acta Crystallogr.*

(12) Dimroth, K.; Reichardt, C.; Siepmann, T.; Bohlmann, F. *Justus Liebigs Ann. Chem.* 1963, 661, 1.

(13) See, for example, Albert, A.; Serjeant, E. P. *The Determination of Ionization Constants*, 3rd ed.; Chapman and Hall: New York, 1984; p 70.

(14) Mataga, N.; Kabota, T. *Molecular Interactions and Electronic Spectra*; Marcel Dekker: New York, 1970; p 293.

Table II. Fluorescence Data for *N*-Purin-6-ylpyridinium Chloride in Different Solvents

solvent	species	λ_{\max} , nm	ϕ	τ , ns
H ₂ O	zwitterion	521	0.08	1.6 ^a
	cation	461		
D ₂ O	zwitterion	521	0.14	2.9
	acetone	549		
methanol	zwitterion	537	0.08	1.7
	cation	455		
ethanol	zwitterion	530	0.08	1.2
	cation	453		

^a pH 3.5–9.0.

in both the fluorescence quantum yield and the excited-state lifetime of the zwitterion on substituting D₂O for H₂O (cf. Table II).

The quantum yield of fluorescence, ϕ_0' , in H₂O at 3 < pH < 9 is 0.08 and the lifetime, τ_0' , is 1.6 ns. One can use these values to calculate the radiative (k_r') and the sum of the first-order or pseudo-first-order nonradiative ($\sum k_{nr}'$) rate constants for the decay of the excited zwitterion by using the relationships¹⁵ $k_r' = \phi_0'/\tau_0'$ and $\sum k_{nr}' = (1 - \phi_0')/\tau_0'$. The results give $k_r' = 5 \times 10^7$ s⁻¹ and $\sum k_{nr}' = 6 \times 10^8$ s⁻¹. The value of k_r' is in good agreement with the value of $k_r' = 6 \times 10^7$ s⁻¹ calculated from the absorption spectrum of the zwitterion by using the Strickler–Berg method.¹⁶ For D₂O, $k_r' = 5 \times 10^7$ s⁻¹ and $\sum k_{nr}' = 3 \times 10^8$ s⁻¹ so that deuteration is seen to affect only the nonradiative disappearance of the excited zwitterion, as expected.

Figure 4 shows that the intensity of the fluorescence of the zwitterion at $\lambda = 521$ nm decreases with decreasing pH at pH < 3, and that a new, blue-shifted emission band appears in the spectrum. Concomitantly, the fluorescence decays become non-exponential. The data are satisfactorily modeled by a biexponential decay function in which the longer lived component decreases monotonically from 1.6 ns at pH > 3 to ca. 0.6 ns at pH 0. The shorter lived component ($\tau \sim 0.1$ ns) is a minor contributor (fraction, $F \leq 0.1$) to the emission at all pHs. However, the fluorescence becomes more complex than biexponential at still lower pHs where the absorption spectra indicate that ground-state protonation to form a dication is occurring. The lifetimes are independent of monitoring wavelength (480–590 nm) in the 0 < pH < 3 range, and no evidence was found for one component growing in as the other decayed (although it would have been impossible to detect the growth of a weak, short-lived component).

When excitation occurs at the isosbestic point wavelength ($\lambda = 316$ nm in aqueous solution, cf. Figure 1), a clear isoemissive point occurs at 450 nm in the emission spectra. This suggests that a proton-transfer reaction also occurs in the excited state, with the emission from the excited cation lying at shorter wavelengths than that of the excited zwitterion. If one assumes that the emission from the cation is negligible at $\lambda > 650$ nm, the low-pH emission spectrum can then be deconvoluted into two components (cf. Figure 4). The low-pH spectrum is first scaled to the same intensity as that found at neutral pH in the $\lambda > 650$ nm range. Subtracting the latter from the former over the whole spectrum then yields a blue-shifted emission with $\lambda_{\max} = 461$ nm, which we ascribe to fluorescence from the excited cation.

Assuming that equilibrium is established, the excited-state pK_a^* value may be calculated by the Förster cycle method.¹⁷ For dilute solutions in which the entropies of (the proton transfer) reaction are equal in the ground and excited states, the excited- and ground-state pK_a 's are related via eq 1, where $\bar{\nu}_{\text{BH}^+}$ and $\bar{\nu}_{\text{B}\pm}$ are

$$pK_a^* = pK_a - hc/2.303kT (\bar{\nu}_{\text{BH}^+} - \bar{\nu}_{\text{B}\pm}) \quad (1)$$

the wavenumbers of the 0–0 electronic transitions of the cation

and the zwitterion, respectively, and the other symbols have their usual meanings. The absorption and emission spectra exhibit no vibrational structure. Therefore $\bar{\nu}_{\text{BH}^+}$ and $\bar{\nu}_{\text{B}\pm}$ were obtained by averaging the frequencies of the maxima of the absorption and emission bands ascribed to the cation and the zwitterion, respectively (cf. data in Tables I and II). This procedure introduces an additional uncertainty into the pK_a^* calculation since this determination of the frequencies relies upon the existence of an exact mirror-image relationship between the absorption and the emission spectra of both species. Nevertheless, this procedure gives a value of $pK_a^* = 0.4 \pm 0.3$, which is in excellent agreement with the value of 0.6 ± 0.1 obtained from the zwitterion–acid fluorescence titration curve, as shown in Figure 5. (We note, however, that both procedures rely on the assumption that equilibrium is in fact established between the excited cation and the excited zwitterion.¹⁸) The large difference between pK_a and pK_a^* (6 orders of magnitude) is ascribable to greatly increased intramolecular charge transfer in the excited singlet state compared with the ground state. Large changes in pK_a on excitation are common among heterocyclic molecules.^{14,18–22}

We can now draw the following conclusions regarding the ground- and excited-state processes occurring in various pH ranges.

(i) 3 < pH < 6. The ground state consists of the cationic form almost exclusively. Excitation of the cation at $\lambda = 290$ –300 nm results in rapid, quantitative deprotonation in the excited state to give the excited zwitterion as the only fluorescent species. Cation deprotonation must occur on a subnanosecond time scale ($k_{\text{rwd}} > 10^{10}$ s⁻¹).

(ii) 6 < pH < 9. The ground state consists of an equilibrium mixture of cation and zwitterion, with the zwitterion predominant at pH > 8. Excitation at all wavelengths spanning the near-UV–vis absorptions of these two species again results in emission from only the excited zwitterion. The lifetime of the excited zwitterion remains constant at 1.6 ns in aqueous solutions over the entire 3 < pH < 9 range.

(iii) 1 < pH < 3. The ground state consists of the cationic form almost exclusively, but both the total intensity of the emission and the lifetime of the major fluorescing species decrease with increasing acidity. Concomitantly, λ_{\max} of the emission shifts to shorter wavelengths, a weaker emission lying to the blue of that due to the zwitterion grows in, an isoemissive point appears at ca. 450 nm, and a minor shorter-lived component of the emission appears. We conclude that the blue-shifted emission is due primarily to the excited cation. However, the weak, shorter lived component in the fluorescence decay ($\tau \sim 100$ ps, $F \leq 0.1$) cannot be ascribed to the excited cation if the photostationary state is established in a time that is short in comparison with the lifetimes of the electronically excited species. We recall that the excited-state cation \rightarrow zwitterion reaction is rapid, and the fluorescence decay of the longer lived component is independent of observation wavelength over the range encompassing emission from both the cation and the zwitterion. We therefore attribute the longer lived component of the fluorescence to the coupled excited cation (acid)–zwitterion (base) pair. The decrease in the total intensity of the emission and the lifetime of the longer lived component with decreasing pH in this range must therefore be due to diabatic proton quenching of the excited zwitterion. Thus, true excited-state equilibrium cannot be established,²³ and the values of the apparent pK_a^* calculated from the Förster cycle and the fluorescence titration curve will be, in this case, somewhat too large (vide infra). The short-lived component of the fluorescence in the low pH range is of unknown origin, but could be associated with, or result from, the occurrence of the ground-state protonation, which is evident in the absorption spectra at high acidity.

(18) Ireland, J. F.; Wyatt, P. A. H. *Adv. Phys. Org. Chem.* **1976**, *12*, 131.(19) Schulman, S. G. In *Modern Fluorescence Spectroscopy*; Wehry, E. L., Ed.; Plenum: New York, 1976; Vol. 2, p 239 ff.(20) Swaminathan, M.; Dogra, S. K. *J. Am. Chem. Soc.* **1983**, *105*, 6223.(21) Mishra, A. K.; Dogra, S. K. *J. Chem. Soc., Perkin Trans. 1* **1984**, 943.(22) Hagopian, S.; Singer, L. A. *J. Am. Chem. Soc.* **1985**, *107*, 1874.(23) Shizuka, J. *Acc. Chem. Res.* **1985**, *18*, 141.(15) Birks, J. B. *Photophysics of Aromatic Molecules*; Wiley-Interscience: New York, 1970; p 142 ff.(16) Strickler, S. J.; Berg, R. A. *J. Chem. Phys.* **1962**, *37*, 814.(17) Förster, T. *Z. Elektrochem. Angew. Phys. Chem.* **1950**, *54*, 42; **1950**, *54*, 531.

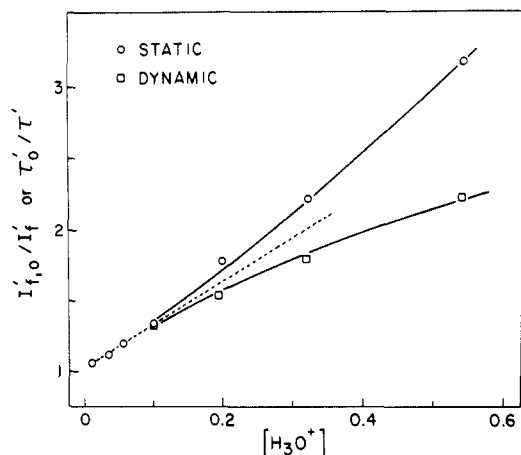


Figure 7. The steady-state and time-dependent Stern–Volmer plots for proton-transfer quenching of excited PuPy⁺. The dashed line gives the initial slope.

We now examine the matter of the quenching of the excited zwitterion by protons in the pH < 3 range. If quenching occurs solely by means of diabatic proton (or H₃O⁺ or H₉O₄⁺) reaction with the excited zwitterion in a process that competes with “normal” radiative and radiationless decay, then the Stern–Volmer relationship may be used^{18,23} to obtain the quenching rate constant, k_q , via eq 2. Here ϕ'_0 and τ'_0 refer to the fluorescence quantum

$$\phi'_0/\phi' = \tau'_0/\tau' = 1 + k_q\tau'_0[\text{H}_3\text{O}^+] \quad (2)$$

yield and the lifetime of the excited zwitterion in the absence of significant proton quenching, i.e. at pH > 3, and ϕ' and τ' refer to the same quantities in the pH < 3 range where significant quenching occurs. Note that ϕ'_0/ϕ' is equal to the ratio of the intensities of fluorescence, $I_{f,0}'/I_f'$. The appropriate plots are shown in Figure 7.

With increasing acid concentration, the fluorescence yield of the zwitterion decreases more rapidly (upward curvature) than the lifetimes (downward curvatures). Such behavior is usually indicative of static quenching or ground-state complexation.¹⁴ In this case, however, we propose that the observed behavior is due to dication formation as a result of a second protonation, most probably on the N3 purine ring nitrogen of PuPy⁺, at higher acid concentrations. Such a protonation is quite reasonable in view of the observed change in the absorption spectrum of PuPy⁺ in 3 M perchloric acid, where the CT band disappears almost completely (cf. Figure 1, inset).

Taking the initial slopes of the plots and the lifetime, $\tau'_0 = 1.6$ ns, yields a value of $k_q = 2.0 \times 10^9 \text{ M}^{-1} \text{ s}^{-1}$ for the proton quenching of the fluorescence of the excited zwitterion. Such a value is reasonable and is quite similar to those observed for the quenching of NH₂, OH, and OCH₃ substituted naphthalenes,²³ which lie in the $(0.75\text{--}8.9) \times 10^9 \text{ M}^{-1} \text{ s}^{-1}$ range. We note, however, that whereas proton quenching dominates the excited neutral decay in the low pH region of the substituted naphthalenes, it occurs at a rate that is only comparable to the excited-state interconversion and decay rates in PuPy⁺. The pseudo-first-order rate constant $k_q[\text{H}_3\text{O}^+]$ takes on a value of $2 \times 10^9 \text{ s}^{-1}$ at pH 0. The values of k_r' and $\Sigma k_{nr}'$ are $5 \times 10^7 \text{ s}^{-1}$ and $6 \times 10^8 \text{ s}^{-1}$, respectively, in aqueous solution. If we take the apparent value of $\text{p}K_a^* \sim 0.5$ as a first approximation to the true equilibrium value of $\text{p}K_a^*$, we estimate $K_a^* \sim 0.3 \sim k_{fwd}/k_{rev}$. Using the previously estimated lower limit for $k_{fwd} > 10^{10} \text{ s}^{-1}$, we find that $k_{rev} > 3 \times 10^9 \text{ s}^{-1}$. It is therefore reasonable that excited-state proton quenching should take place in the low pH region but will not dominate except at pH < 0. The excited-state $\text{p}K_a^*$'s estimated from the Förster cycle (0.4) and the fluorescence titration (0.6) should thus be reasonably good first approximations to the true value. To our knowledge this is the first report of a singlet excited state $\text{p}K_a^*$ value for a purine.

3. Fluorescence of Nonaqueous Solutions. The fluorescence spectra of PuPy⁺ in methanol and acetonitrile show a concentration

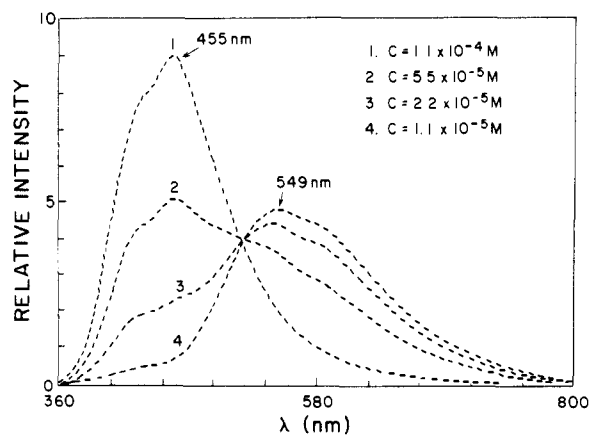


Figure 8. Concentration dependence of the fluorescence spectra of PuPy⁺ in acetonitrile. The spectra are corrected for the changes in absorbance with concentration at λ_{ex} .

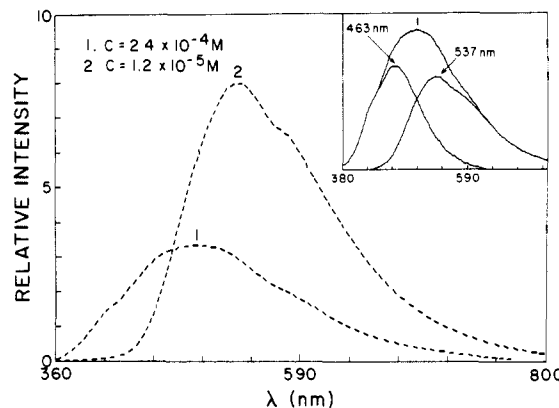


Figure 9. Concentration dependence of the fluorescence spectra of PuPy⁺ in methanol. Spectra are corrected for the changes in absorbance with concentration at λ_{ex} . Inset, spectrum 1 deconvoluted into cation ($\lambda_{\text{max}} = 463 \text{ nm}$) and zwitterion ($\lambda_{\text{max}} = 537 \text{ nm}$) emissions.

dependence similar to that observed in their absorption spectra (cf. Figures 8 and 9). In acetonitrile solution, at concentrations where both cation and zwitterion are present, the excitation and absorption spectra do not match. The excitation spectra are a function of the wavelength at which the emission is observed and correspond to the absorptions of the separate ionic species when the emission wavelength is chosen appropriately. We conclude that the observed changes in the fluorescence spectra with concentration are due solely to the operation of a ground-state equilibrium.

Excitation of the methanolic solutions in which only the cationic species are present results in a broad emission spectrum. Fluorescence decay measurements reveal the existence of two components having lifetimes of 400 ps and 1.7 ns, which, in this case, can be ascribed to the unequilibrated cation and zwitterion, respectively. The fluorescence spectrum of the cationic species was obtained in a manner similar to that for aqueous solution by subtracting the emission of the zwitterion from the spectrum containing the sum of the emissions of the two species (cf. Figure 9, inset). We note here, parenthetically, that the fluorescence yields and lifetimes of PuPy⁺ in alcohols and acetonitrile are highly dependent upon the water content of these solvents. However, the implications of this observation are beyond the scope of the present work and will be the subject of further, detailed study.

In 95% ethanol, acidified to pH 4 so that only the cationic form is present in solution, the fluorescence results almost exclusively from the zwitterion. This probably reflects the effect of increased water concentration on the proton-transfer reaction in the excited state.²⁴ Lowering the temperature of this solution results in a blue shift of the emission and a gradual increase in the fluorescence

(24) Lee, J.; Griffin, R. D.; Robinson, G. W. *J. Chem. Phys.* 1985, 82, 4920.

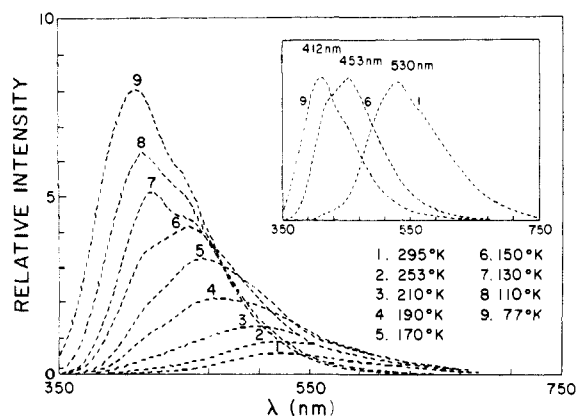


Figure 10. The temperature dependence of the fluorescence of PuPy⁺ in 95% ethanol. Inset, spectra 1, 6, and 9 normalized at λ_{\max} .

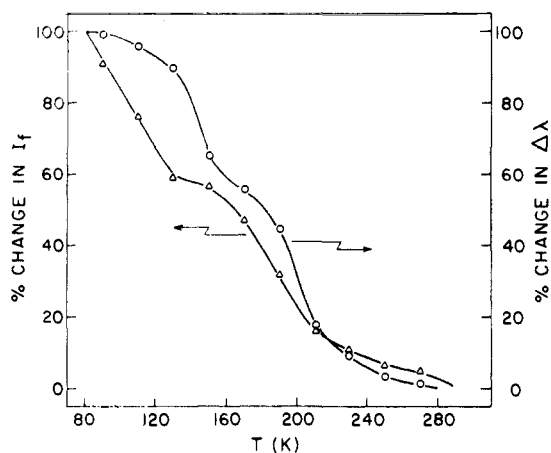


Figure 11. Plots of fluorescence intensity (Δ) and shift of λ_{\max} (O) in ethanol vs temperature.

intensity (cf. Figure 10). The plots of $\Delta\lambda_{\text{em}}$ and ΔF vs temperature (Figure 11) are similar, and both resemble the fluorescence titration curves. It is possible that the sigmoidal portion of the curve of Figure 11 between 280 K and ca. 160 K may be associated with the excited-state proton-transfer reaction, whereas the remaining portion of the curve from 160 K to 77 K might be attributed to a change in the rate of orientational relaxation of the solvent around the excited molecules. If this interpretation is valid, the spectrum at 150 K corresponds to emission from the equilibrated, excited singlet state of the cation, whereas at 77 K the reorientation of the polar solvent is too slow to compete with the decay process, and the spectrum corresponds to emission from the (solvent) unequilibrated singlet state of the cation.

The fluorescence data for PuPy⁺ are summarized in Table II. Note that solvatochromism similar to that in absorption occurs also in the fluorescence spectra. However, the differences in λ_{\max} between the two species in the same solvent are much larger in fluorescence than in absorption, while the blue shifts of the fluorescence maxima for a given species in water are smaller than those in absorption. The above observations lead to the following conclusions. First, the fluorescence of PuPy⁺ originates from a π, π^* singlet state having considerable CT nature. Second, excitation leads to a substantial decrease in the polarity of the molecule. Third, the extent of the intramolecular CT interaction is significantly greater in the zwitterion than the cation (increased electron-donating ability of the donor) and becomes greater in the excited state for both the cation and the zwitterion.

4. Fluorescence Quenching. The quenching of PuPy⁺ fluorescence by iodide ions (in the form of NaI) at 0.5 M total ionic strength (adjusted with NaClO₄) was studied in aqueous solutions at pH 3.5 and 8.0. The primary motivation for doing this experiment was to examine the effect of quenching by a counterion on the proton transfer from the excited cation (pH 3.5)

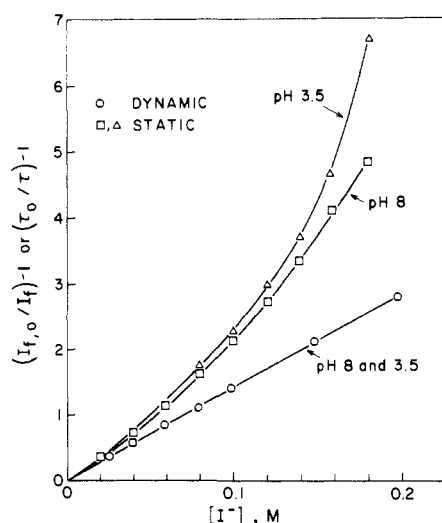


Figure 12. The steady-state and time-dependent Stern-Volmer plots for fluorescence quenching of PuPy⁺ by NaI at various pHs.

and to compare the quenching rate with that for the quenching of the excited zwitterion, which can be formed directly from the ground state at pH ≥ 8 . The relevant Stern-Volmer plots are shown in Figure 12. Note that plots constructed from the lifetimes (dynamic) are linear and independent of pH whereas those constructed from the steady-state fluorescence intensities (static) show significant upward curvature. The latter observation is indicative of a substantial contribution of static quenching to the overall quenching process at high iodide concentrations. Association of iodide ion with both the ground-state cation and zwitterion is implied. The departure from linearity is slightly more pronounced at pH 3.5, and we attribute this to stronger interaction between the cation and the iodide anion than between the zwitterion and iodide, as is reasonable on electrostatic grounds.

The slope of the (dynamic) Stern-Volmer plot gives $k_q\tau = 14.3 \text{ M}^{-1}$. The fact that exactly the same slope is obtained both at pH 3.5 (where the cation is predominant in the ground state) and at pH 8.0 (where the zwitterion is predominant in the ground state) indicates either (i) that the dynamic quenching of both the excited cation and the excited zwitterion by iodide anion occur at the same rate or (ii) that the excited cation dissociates at a rate that is rapid compared with the rate of quenching. The former seems unlikely on electrostatic grounds, so we conclude that the latter applies. Thus the fluorescence, which is quenched at pH 3.5, is that of the excited zwitterion, whose unquenched lifetime is 1.6 ns. A value of $k_q = 8.9 \times 10^9 \text{ M}^{-1} \text{ s}^{-1}$ is therefore calculated, which is near the diffusion-controlled limit for neutral species.²⁵ At the highest iodide concentration employed, 0.2 M, $k_q[\text{I}^-] \sim 2 \times 10^9 \text{ s}^{-1}$, which must be substantially smaller than k_{fwd} for the deprotonation of the excited cation. A value of $k_{\text{fwd}} > 10^{10} \text{ s}^{-1}$ is implied, in agreement with our previous conclusions.

Conclusion

The photophysical and spectroscopic properties of PuPyCl in aqueous solutions at $0 < \text{pH} < 10$ and in methanol, ethanol, and acetonitrile have been studied. In aqueous solutions, excitation of either the ground-state cation or the ground-state zwitterion in the $3 < \text{pH} < 9$ range ($\text{p}K_a = 6.7$) results in emission from the excited zwitterion exclusively. This emission is characterized by a fluorescence quantum yield, $\phi_0' = 0.08$ and a single exponential decay time, $\tau_0' = 1.6 \text{ ns}$. Rapid ($k_{\text{fwd}} > 10^{10} \text{ s}^{-1}$) proton transfer from the excited cation to the solvent is inferred. At $0 < \text{pH} < 3$ diabatic proton quenching of the excited zwitterion occurs with rate constant $k_q = 2 \times 10^9 \text{ M}^{-1} \text{ s}^{-1}$, but this is not sufficiently large to cause the photostationary state to differ greatly from the true excited state phototropic equilibrium state. The Förster cycle and fluorescence titration yield values of $\text{p}K_a^* =$

(25) Lakowicz, J. R. *Principles of Fluorescence Spectroscopy*; Plenum: New York, 1983; p 258.

0.4 ± 0.3 and 0.6 ± 0.1, respectively. Preliminary indications are that the excited-state equilibrium is not established as rapidly in methanol and ethanol.

These and other preliminary results²⁶ indicate that pyridinium salts may very well serve as useful fluorescent probes for nucleic acids and perhaps other biomolecules. The pyridinium salt derived from hypoxanthine has a zwitterion which dominates the ground-state prototropic equilibrium at pH > 6.7. It possesses a strong charge-transfer absorption band which is considerably red-shifted from the main UV absorption systems of the purines and pyrimidines. The excited zwitterion fluoresces moderately strongly, and the emission spectra and lifetimes are invariant over a wide pH range (3 < pH < 9 for PuPyCl), including the physiological region. This, together with the high degree of photostability of this particular system in aqueous solution, also suggests that it might find utility as a fluorescence standard. Preliminary work²⁶ indicates that other similar compounds may exhibit substantially larger fluorescence quantum yields. Transformation of hypoxanthine and other purine bases into pyridinium salts is straightforward.^{7,8}

Experimental Section

Materials. *N*-Purin-6-ylpyridinium chloride was synthesized and purified according to the general procedure used previously for the synthesis of other nucleobase-derived pyridinium salts.^{7,8} Thus, hypoxanthine (0.680 g, 5 mmol) was reacted with 4-chlorophenyl phosphorodichloridate (2.8 mL, 15 mmol) to give 0.790 g of the desired compound. Yield: 68%. Mp > 300 °C dec. MS: *m/e* (relative intensity) 197 (2.6) (M - HCl)⁺, 79 (100) Py⁺. NMR (D₂O): δ_H 10.03 (2 H, d, *J* = 5.8 Hz), 9.13 (1 H, s), 8.94 (1 H, t, *J* = 8 Hz), 8.80 (1 H, s), 8.43 (2 H, t, *J* = 7.5 Hz). Anal. Calcd for C₁₀H₈N₅Cl: C, 51.4; H, 2.3; N, 30.0. Found: C, 51.2; H, 2.4; N, 29.7.

HClO₄, NaClO₄, NaI, and D₂O were used as received. Spectrograde ethanol (Merck) and HPLC grade methanol and acetonitrile (both BDH

Omnisolv) were used without further purification. Water was purified by using a Millipore Super-Q system. The samples used in the fluorescence measurements were prepared by volume from stock solutions of the fluorophore, HClO₄, NaI, and NaClO₄, so as to maintain a constant ionic strength.

Methods. The electronic absorption, excitation, and emission spectra were recorded on a Cary 118 spectrophotometer and a Spex Fluorolog 222 spectrofluorometer. All experiments, except for the temperature dependence of fluorescence in ethanol, were carried out at room temperature on aerated solutions. Fluorescence yields were determined relative to quinine bisulfate ($\phi_f = 0.55$ 1 N H₂SO₄²⁷). A DN70 low-temperature cell and MTIC temperature control unit, both from Oxford Instruments, were used for fluorescence measurements between 293 and 77 K.

Fluorescence lifetime measurements were made on the picosecond laser system described previously²⁸ by using the single photon counting technique. The samples were excited at 297 nm, and emission was monitored at 461 and 521 nm, corresponding to the maxima in the deconvoluted emission spectra of the cation and zwitterion (Figure 4). Fluorescence decay curves were analyzed by the excitation pulse shape mimic technique developed earlier in this laboratory.²⁸ The mimic chosen was 4-bromo-2,2,3,3-tetramethylindanthione in pentane ($\tau < 100$ ps).²⁹ The χ^2 values were within 1.0–1.1 for single-exponential fits and did not exceed 1.3 for double-exponential decays. The errors for the lifetimes presented in this paper are no more than 3–5% for the longer-lived decays and are less than 15% for the short-lived components.

Acknowledgment. We thank the Natural Sciences and Engineering Research Council of Canada for financial support. B.S. thanks the President's NSERC fund of the University of Saskatchewan for providing the postdoctoral fellowship, A. Mickiewicz University for allowing a leave of absence, and Prof. S. Paszyc and Dr. R. W. Adamiak for their interest in this work. Partial support within the project R.P. II. 13.2.15 is also acknowledged.

(26) Skalski, B.; Steer, R. P.; Verrall, R. E.; Paszyc, S.; Adamiak, R. W. Proceedings, XIII International Conference on Photochemistry; Budapest, 1987; Abstracts; Vol. II, p 404.

(27) Demas, J. N.; Crosby, G. A. *J. Phys. Chem.* **1971**, *75*, 991.

(28) James, D. R.; Demmer, D. R. M.; Verrall, R. E.; Steer, R. P. *Rev. Sci. Instrum.* **1983**, *54*, 1121.

(29) Maciejewski, A.; Szymanski, M.; Steer, R. P., unpublished results.

H_xMoO₃ Bronzes: Structures, Stabilities, and Electronic Properties

S. P. Mehandru and Alfred B. Anderson*

Contribution from the Chemistry Department, Case Western Reserve University, Cleveland, Ohio 44106. Received June 18, 1987

Abstract: An atom superposition and electron delocalization molecular orbital study has been made of H⁺ adsorption on MoO₃. Band structures, geometries, binding energies, force constants, and stretching frequencies have been calculated. It is predicted that H⁺ adsorbs most strongly on the basal plane O²⁻ for the low as well as high hydrogen content H_xMoO₃ bronze. For the higher hydrogen content bronze, earlier suggestions in the literature that OH₂ groups are formed are confirmed. Once on the basal planes between the layers, hydrogen is expected to diffuse easily at high temperatures. On the edges of the crystal layers, the most stable chemisorption form is heterolytic, with H⁺ bonded to O²⁻ and H⁻ bonded to Mo^V.

A variety of bronzes, A_xMO₃ where M = W, Mo, Re and A = Na, K, Rb, Cs, NH₄, Ca, Sr, Ba, etc., are found to be superconductors with critical temperatures as high as 6 K.¹ Hydrogen bronzes have been used as heterogeneous catalysts for the hydrogenation of NO₂ and alkenes,³ where they act as hydrogen

reservoirs. Color changes often accompany bronze formation and this property has been investigated in connection with their use as electrochromic devices for displays.⁴ The effect of hydrogen

(1) (a) Sweedler, A. R.; Raub, C.; Matthias, B. T. *Phys. Lett.* **1965**, *15*, 108. (b) Sweedler, A. R.; Hulm, J. K.; Matthias, B. T.; Geballe, T. H. *Phys. Lett.* **1965**, *19*, 82. (c) Bierstedt, P. E.; Bither, T. A.; Darnell, F. J. *Solid State Commun.* **1966**, *4*, 25. (d) Gier, T. E.; Pease, D. C.; Sleight, A. W.; Bither, T. A. *Inorg. Chem.* **1968**, *7*, 1646. (e) Sleight, A. W.; Bither, T. A.; Bierstedt, P. E. *Solid State Commun.* **1969**, *7*, 299.

(2) (a) Glemser, O.; Lutz, G. Z. *Anorg. Allg. Chem.* **1951**, *264*, 17. (b) Glemser, O.; Hauschild, U.; Lutz, G. Z. *Anorg. Allg. Chem.* **1952**, *269*, 93.

(3) (a) Sermon, P. A.; Bond, G. C. *Catal. Rev. Sci. Eng.* **1973**, *8*, 211. (b) Bond, G. C.; Sermon, P. A.; Tripathi, J. B. P. *Ind. Chim. Belge* **1973**, *38*, 506. (c) Sermon, P. A.; Bond, G. C. *J. Chem. Soc., Faraday Trans.* **1980**, *76*, 889. (d) Marq, J. P.; Wispeninckx, X.; Poncelet, G.; Keravis, D.; Fripiat, J. J. *J. Catal.* **1982**, *73*, 309. (e) Marq, J. P.; Poncelet, G.; Fripiat, J. J. *J. Catal.* **1984**, *87*, 339.

(4) (a) Chang, I. F.; Gilbert, B. L.; Sun, T. I. *J. Electrochem. Soc.* **1975**, *122*, 955. (b) Reichman, B.; Bard, A. J. *J. Electrochem. Soc.* **1979**, *126*, 2133. (c) Gottesfeld, S.; McIntyre, J. D. E. *J. Electrochem. Soc.* **1979**, *126*, 742, 2171.